RSC Advances

REVIEW

View Article Online
View Journal | View Issue

Cite this: *RSC Adv.*, 2016, **6**, 32598

Amine-functionalized metal–organic frameworks: structure, synthesis and applications

Yichao Lin, Chunlong Kong and Liang Chen*

We present a review on some recent studies on the syntheses, structures and properties of amine-functionalized metal–organic frameworks (MOFs), and highlight the benefits of amino functionality towards potential applications. Owing to the strong interaction between CO_2 and basic amino functionalities, amine-functionalized MOFs have attracted much attention mainly for CO_2 capture. Besides the most widely used *in situ* synthesis method, post-modification and physical impregnation methods are developed to prepare amine-functionalized MOFs with extremely high CO_2 sorption capacity at low pressures. On the basis of the similar mechanism, amine-functionalized MOF-based membranes, including pure amine-functionalized MOF membranes and mixed matrix membranes, exhibit excellent CO_2/H_2, CO_2/CH_4 and CO_2/N_2 separation performance. Furthermore, amine-functionalized MOFs also demonstrate potential applications in catalysis.

Received 18th January 2016
Accepted 21st March 2016

DOI: 10.1039/c6ra01536k

www.rsc.org/advances

1. Introduction

In recent decades, the family of metal–organic frameworks (MOFs) or porous coordination polymers (PCPs) has been extensively explored by chemists, physicists and materials scientists owing to their striking chemical and physical properties.[1–3] These interesting MOF materials are organic–inorganic hybrid porous solids built from organic linkers and inorganic metal nodes. To date, the interest on MOFs mainly comes from their high surface areas (up to 8000 $m^2\ g^{-1}$), permanent porosity and tunable pores. These traits make them very promising candidates for gas storage and separation, drug delivery, catalysis and sensing or recognition.[4] Notably, the syntheses of MOF-5 and HKUST-1 have been scaled up recently by BASF in collaboration with Yaghi's group and used in natural gas vehicles to increase fuel storage capacity.[1]

As a new class of porous materials, MOFs diverge from the traditional zeolites in many aspects.[2] For example, MOFs possess larger flexibility in composition and less topological constraints in the formation of frameworks, which have given birth to more than 20 000 MOF structures.[1] Hence, MOFs family is foreseen as the next-generation leading porous materials. Recently, much attention has been recently devoted on MOFs consisting of functional groups, so that some desirable chemical and physical properties can be imparted. To date, a series of functionalized MOFs[5–9] containing different functional groups

Ningbo Institute of Materials Technology & Engineering, Chinese Academy of Sciences, 1219 Zhongguan West Road, Zhenhai District, Ningbo, PR China. E-mail: chenliang@nimte.ac.cn

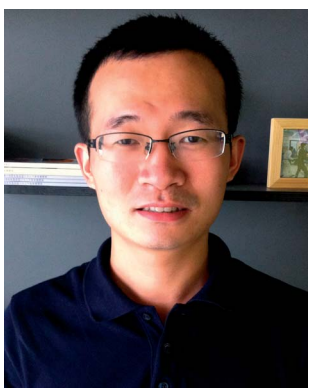

Dr Yichao Lin obtained his Ph.D. in physical chemistry of materials from Ningbo Institute of Materials Technology and Engineering (NIMTE), Chinese Academy of Science in 2015. Currently, he is a post-doctoral fellow at NIMTE with Prof. Liang Chen. His research interests include the synthesis and development of functionalized metal–organic frameworks for CO_2 capture and energy storage.

Dr Chunlong Kong is an associate professor in the Ningbo Institute of Material Technology and Engineering, Chinese Academy of Science. He obtained his Ph.D. in chemistry from Dalian University of Technology, under the supervision of Prof. Jinqu Wang. He then did post-doctoral studies with Prof. Toshinori Tsuru at the Department of Chemical Engineering, Hiroshima University. His current research focuses on the design of porous materials for gas separation, storage and catalysis.

(*e.g.*, –OH, –NH_2 and –Br) has been prepared and characterized. Among them, amine-functionalized MOFs are the most investigated mainly because of their basic amine groups, which display strong affinity to acidic gas molecules and can render active sites for catalysis. Moreover, amine-functionalized MOFs can serve as a good platform for post synthetic modification (PSM). This review will focus on the amine-functionalized MOFs reported to date, including the amino functionalities on organic linkers or metal sites. In addition, the MOFs with polyamines constrained in pores are also reviewed. We will first summarize some recent progresses on the syntheses for amine-functionalized MOFs, and then we will introduce their potential applications and finally draw some conclusions.

2. Synthesis of amine-functionalized MOFs

Currently, amine-functionalized MOFs are prepared mainly by following three routes: (i) *in situ* synthesis, (ii) post-modification with amines and (iii) physical mixing unfunctionalized MOFs and polyamines. Among these routes, the *in situ* synthesis method is the mostly used. The other methods have been developed and investigated only recently. Fig. 1 shows the structures/cages of amine-functionalized or their parent frameworks *via in situ* synthesis.

2.1 *In situ* synthesized amine-functionalized MOFs

2.1.1 Amine-functionalized MOFs with structure motif. Hydrothermal/solvothermal synthesis, which employs high temperatures and elevated pressures, is by far the most successfully used method for *in situ* preparation of MOFs.[4,10,11] However, under solvothermal conditions, thermally labile functional groups of ligands will coordinate metal ions, resulting in undesired solids and inhibiting MOF assembly. Therefore, MOFs with chemical functionality are very limited,[12] although numerous MOFs have already been reported. Interestingly, the majority of functionalized MOFs consist of amine-functionalized MOFs (Table 1).

To our knowledge, MOF-46,[13] constructed by the 2-amino-1,4-benzenedicarboxylate (NH_2BDC) linkers and Zn ions, is the first reported amine-functionalized MOF with robust three-dimensional (3D) framework. MOF-46 was initially designed from the structural motif of MOF-2 which is constructed by paddle-wheel secondary building units (SBUs) and 1,4-benzenedicarboxylate (H) linkers. The substituents on benzene ring are speculated to result in rotation of carboxylate out of the benzene ring plane. In this regard, the framework can be changed or even disrupted if some unsuitable substituents are introduced onto the benzene ring. The authors found that the distance (*d*) between the substituents of linkers of the same paddle-wheel is an important parameter for the designed structure (Fig. 2). The value of *d* should not be larger than the sum of the van der Waals radius of two functional groups. Otherwise, the designed functionalization cannot be obtained. This condition explains why amine-functionalized MOF-2 (MOF-46) was successfully synthesized, whereas methyl-functionalized MOF-2 cannot be synthesized.

Another amine-functionalized MOF, IRMOF-3 (ref. 14) (Isoreticular Metal–Organic Frameworks-3), which was *in situ* synthesized, is one of the most fully investigated functionalized MOFs due to its high porosity, excellent stability, crystalline structure and accessible amino groups on the benzenedicarboxylate (BDC) linker. The crystalline structure of IRMOF-3 is generally identical to that of IRMOF-1 (also known as MOF-5), which is a starting structural motif. It has a rigid cubic framework constructed by Zn_4O SBUs and NH_2BDC rods. IRMOF-3 can be synthesized by a mixture of zinc nitrate tetrahydrate and NH_2BDC in *N*,*N*-diethylformamide (DEF) under solvothermal conditions, *i.e.* similar synthesis condition as that in MOF-5 synthesis. Accordingly, successful IRMOF-3 synthesis can also be explained by the abovementioned rule. Interestingly, the active amine pendants in the IRMOF-3 framework can be further modified by simple covalent reactions, such as acetylation.[15] Owing to its excellent chemical and thermal stability, as well as high porosity,[16] IRMOF-3 is therefore a good model system for PSM.

By using the same method and process, researchers have recently synthesized some attractive amine-functionalized MOF,[17–20] such as NH_2-UiO-66 (ref. 19) (UiO = University of Oslo) and NH_2-MIL-101(Cr).[20] The only difference is that, sometimes, the synthesis temperatures and duration should be adapted because of the accelerating effect of amine groups on crystallization. NH_2-UiO-66 was initially synthesized from the structural motif UiO-66, which is a classical MOF exhibiting an expanded cubic close-packed structure. UiO-66 (ref. 21) was prepared from a mixture of $ZrCl_4$ and H_2BDC under solvothermal conditions in DMF. Simple replacement of H_2BDC by NH_2BDC leads to the formation of crystalline NH_2-UiO-66 under the same solvothermal conditions with a shorter duration. NH_2-MIL-101(Cr) has attracted much attention due to its amine pendant together with very high surface areas, excellent stability against moisture and simple synthesis process. Its parent MIL-101(Cr)[3] was first reported by Ferey and coworkers and rapidly

Prof. Liang Chen received his B.S. in applied chemistry from Nanjing University in 2001 and Ph.D. from the Department of Chemical Engineering at the University of Pittsburgh and National Energy Technology Lab in 2006. He then spent one year as a postdoctoral fellow at Air Products and Chemicals, Inc. working on a hydrogen storage project supported by the US Department of Energy. Currently, he is a professor in Ningbo Institute of Materials Technology and Engineering, Chinese Academy of Sciences. His research is focused on the design and development of novel porous materials for gas sorption, separation and catalysis.

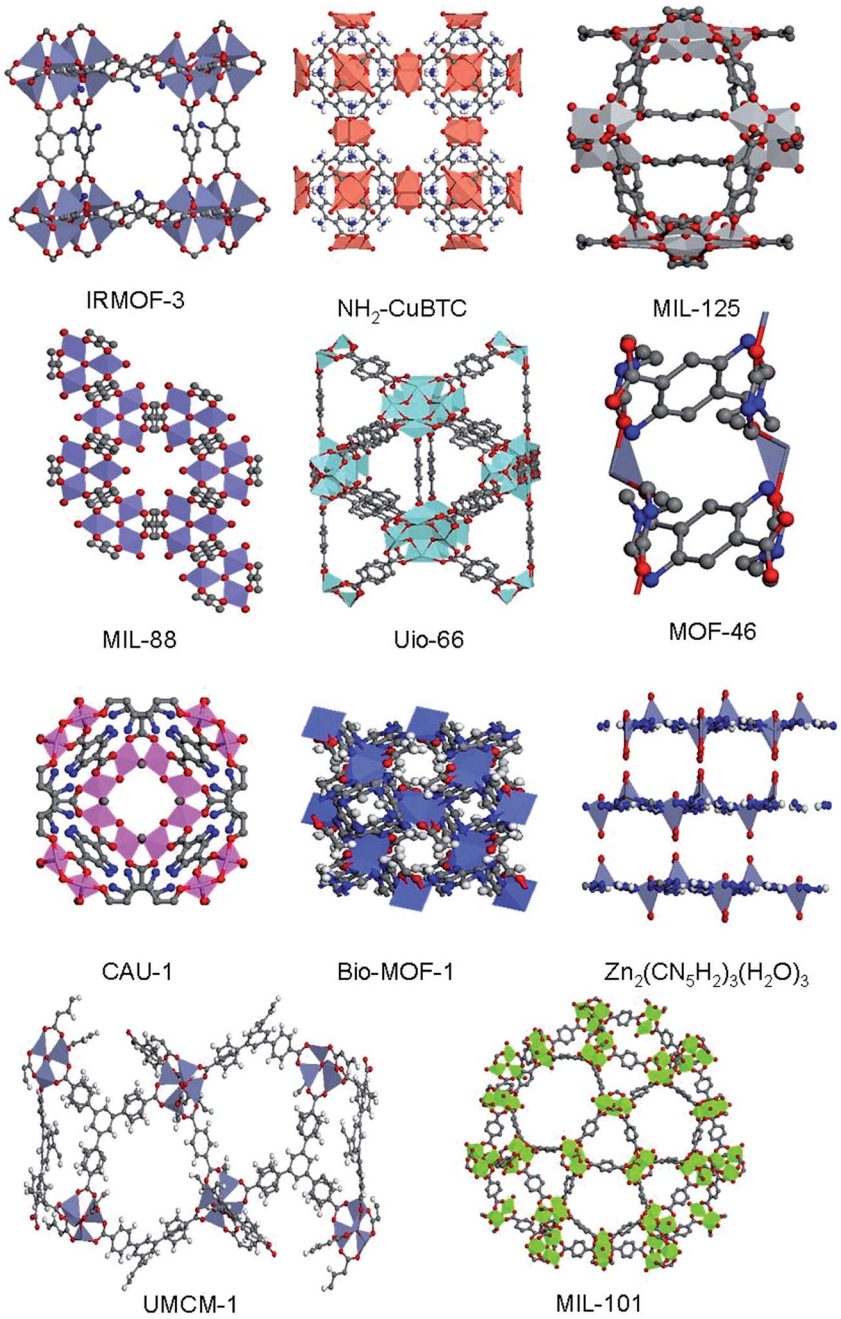

Fig. 1 Structures/cages of amine-functionalized MOFs or their parents.

became one of the most important members of the MOFs family. It possesses mesopores, excellent stability and open metal sites. On the basis of the abovementioned experimental route and taking account of the accelerating effect of amine groups, Chen and coworkers lowered the synthesis temperature and added some base to obtain NH_2-MIL-101(Cr), which shows excellent stability and exhibits a high surface area (up to 1675 $m^2\ g^{-1}$) and a large pore volume (up to 1.67 $cm^3\ g^{-1}$). Burrows and coworkers[22] further reported on the synthesis of NH_2-MIL-101(Cr) and presented a tandem PSM strategy. Another amine-functionalized MOF in the MIL series is NH_2-MIL-125 reported by Li.[23] The structure of NH_2-MIL-125 is similar to that of MIL-125,[24] which is constructed from titanium-oxo-hydroxo clusters and H_2BDC linkers with a quasi-cubic tetragonal structure.

The framework of the abovementioned amine-functionalized MOFs are rigid. Moreover, flexible frameworks are much more attractive because their pore volumes and pore sizes can be adjusted by host–guest interactions. MIL-53 (ref. 25) and MIL-88 (ref. 26) display this structural feature. For instance, the pore channels of MIL-53 filled with water molecules are quite narrow; however, the pore size increased after the water molecules were removed. More importantly, this flexibility transformation is reversible. This interesting phenomenon is thus called "breathing effect". The

Table 1 The reported amine-functionalized MOFs and their structure information

Acronym name	Ligand	$S_{Langmuir}$ ($m^2 g^{-1}$)	S_{BET} ($m^2 g^{-1}$)	V_{pore} ($cm^3 g^{-1}$)	Ref.
MOF-46	2-Amino-1,4-benzenedicarboxylate	—	—	—	13
CAU-1	2-Amino-1,4-benzenedicarboxylate	1700	1268	1.32	36 and 41
IRMOF-3	2-Amino-1,4-benzenedicarboxylate	3062	2446	1.07	16
		—	2850	—	42
UiO-66-NH_2	2-Amino-1,4-benzenedicarboxylate	—	1206	—	19
			1123	0.52	43
MOF-LIC-1	2,4-Diamino-1,4-benzenedicarboxylate	—	—	—	31
UiO-66-NH_2 (mixed linker)	2-Amino-1,4-benzenedicarboxylate	1313	1112	—	5
NH_2-MIL-101(Cr)	2-Amino-1,4-benzenedicarboxylate	2280	1675	—	20
			2070	2.26	22
NH_2-MIL-101(Al)	2-Amino-1,4-benzenedicarboxylate	—	2100	0.77	31
		—	3099	1.53	44
NH_2-MIL-101(Fe)	2-Amino-1,4-benzenedicarboxylate	—	3483	1.64	44
NH_2-MIL-68(In)	2-Amino-1,4-benzenedicarboxylate	—	2160	0.48	45
NH_2-MIL-88(Al)	2-Amino-1,4-benzenedicarboxylate	—	—	—	28
NH_2-MIL-53 (mixed linker)	2-Amino-1,4-benzenedicarboxylate, 1,4-benzenedicarboxylate	—	1000–1100	0.43–0.51	46
NH_2-MIL-53	2-Amino-1,4-benzenedicarboxylate	—	735	0.345	47
Bio-MOF-1	Adenine, biphenyldicarboxylic acid	—	1700	—	39
Bio-MOF-11	Adenine	—	1040	0.45	38
Bio-MOF-100	Adenine, biphenyldicarboxylic acid	—	4300	4.3	40
NH_2-MIL-125	2-Amino-1,4-benzenedicarboxylate	1719	1302	—	23
			1245	0.53	48
$Zn_2(Atz)_2$	3-Amino-1,2,4-triazole	—	782[b]	0.19[b]	35
DMOF-1-NH2	2-Amino-1,4-benzenedicarboxylate, 1,4-diazabicycloctane	—	1510	—	49
UMCM-1-NH_2	2-Amino-1,4-benzenedicarboxylate, 4,4′,4″-benzene-1,3,5-triyl-tribenzoic acid	—	3973	—	49
$Zn_2(CN_5H_2)_3(H_2O)_3 \cdot 6H_2O$	5-Amino-1*H*-tetrazole	433	340.8	—	37
NH_2-CuBTC	2-Amino-1,3,5-benzenetricarboxylate	—	1834	0.69[a]	29
MAF-66	3,5-Diamino-1,2,4-triazole	1196	1014	0.43	34
CPF-13	3,5-Diamino-1,2,4-triazole, 1,4-benzenedicarboxylate	1008	642	—	50
ZnF(Am_2TAZ)	3,5-Diamino-1,2,4-triazole	—	—	—	17

[a] Micropore volume. [b] Calculated from the fit to the density functional theory model.

corresponding amine-functionalized MIL-53(Al, Fe)[27,28] and MIL-88(Fe)[28] were further developed. Owing to the effect of breathing and its amine groups, NH_2-MIL-53(Al) exhibits interesting gas adsorption properties, which will be discussed in the next section.

The formation of desired frameworks is not always controllable during MOF synthesis under solvothermal conditions. The solvent, pH and temperature have profound impact on structure formation. High-throughput method has been used to study the solvothermal reactions of $FeCl_3$ and NH_2BDC.[28] It was found that, different solvents, pH and temperatures resulted in different types of amine-functionalized MOFs: NH_2-MIL-53(Fe), NH_2-MIL-88(Fe), NH_2-MIL-101(Fe) or amorphous solids. In another example, NH_2-CuBTC with pure linker cannot be synthesized in the same condition as that of CuBTC. Instead, Peikert and coworkers successfully synthesized NH_2-CuBTC by using a different solvent.[29] Sometimes, even the type of metal salt source plays a key role in structure formation in MOFs. For example, NH_2-MIL-101(Al)[30] can be synthesized with *via* a reaction between $AlCl_3$ and NH_2BDC in DMF under solvothermal conditions. By contrast, when the metal salt $AlCl_3$ was replaced by $Al(NO_3)_3$, NH_2-MIL-53(Al)[31] was obtained. Another example is NH_2-MIL-88(Sc),[32] which was obtained from a metal salt of $Sc(NO_3)_3 \cdot 3H_2O$ under solvothermal condition. When $Sc(NO_3)_3 \cdot 3H_2O$ was replaced by Sc_2O_3, Sc_2BDC_3 was crystallized. In addition, NH_2-MIL-101(Al) was successfully synthesized, whereas its 'structure motif' MIL-101(Al) has not yet been reported, demonstrating the complexity of structure formation of MOFs.

2.1.2 Amine-functionalized MOFs without structural motif. The above amine-functionalized MOFs possess 'structural motif'. However, some amine-functionalized MOFs have been initially synthesized without structural motif. MOF-LIC-1,[33] MAF-66 (ref. 34) (MAF = metal azolate frameworks), $Zn_2(Atz)_2$,[35] CAU-1 (ref. 36) and $Zn_2(CN_5H_2)_3(H_2O)_3 \cdot 6H_2O$ (ref. 37) belong to this category. MOF-LIC-1 was initially synthesized from the reaction of gadolinium nitrate with 2,4-diamino-1,4-benzene dicarboxylic acid in DMF under solvothermal condition, displayed an octahedral network with infinite pore channels and oriented amino groups. MAF-66 (ref. 34) is constructed by Zn nodes and 3-amino-1,2,4-triazole linkers, possesses a BET surface area of 1014 $m^2 g^{-1}$ and a total pore volume of 0.43 $cm^3 g^{-1}$. $Zn_2(Atz)_2$ was synthesized *via* a solvothermal reaction of zinc carbonate, 3-amino-1,2,4-triazole and oxalic acid.[35] The framework was built from pillaring of Zn-aminotriazolate layers

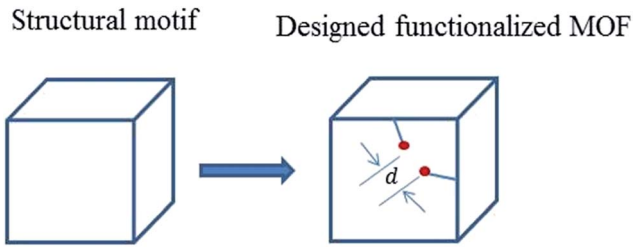

Fig. 2 Schematic representation of the original structural motif and designed functionalized MOF. *d* is the distance between two functional groups.

caused by oxalate groups and exhibited a BET surface area and pore volume of 782 $m^2\ g^{-1}$ and 0.19 $cm^3\ g^{-1}$, respectively. $Zn_2(Atz)_2$ has been comprehensively investigated for its excellent CO_2 capture ability, which will be covered in the next section. CAU-1 is well known for its unprecedented octameric $\{Al_8(OH)_4(OCH_3)_8\}^{12+}$ building units attached to a 12-connected net. CAU-1 displays high porosity with a Langmuir surface area of 1700 $m^2\ g^{-1}$ and high thermal stability. Moreover, $Zn_2(CN_5H_2)_3(H_2O)_3\cdot 6H_2O$ (ref. 37) is an interesting amine-functionalized MOF with two-dimensional layered framework. In the framework, each 5-aminotetrazole ligand is linked to two zinc nodes, resulting in 1D square channels. Each layer is connected by hydrogen bonding, and the free amino groups are accessible and located around the cavities.

In addition, a series of bio-MOFs with amino groups, which is known for their biocompatibility, can be also classified in this category. Bio-MOF-11 (ref. 38) was synthesized *via* a solvothermal reaction between cobalt acetate tetrahydrate and adenine in DMF. Adenine is an ideal biomolecular ligand for constructing bio-MOFs because of its rigidity and multiple metal binding sites. The structure of bio-MOF-11 consists of cobalt–adeninate–acetate paddle-wheel clusters, which can be regarded as the square SBUs, where two Co^{2+} ions are bridged by two adeninates and two acetates. The dimension of cube-shaped space within the framework is approximately 4.0 Å × 4.0 Å × 4.0 Å. The free amine groups of adeninates in the framework and the biocompatibility make the bio-MOFs important members of the amine-functionalized MOFs family. Interestingly, introducing biphenyldicarboxylic acid into the reactions between adenine and zinc acetate dehydrate in DMF lead to the formation of bio-MOF-1.[39] The SBUs of bio-MOF-1 are also the zinc–adeninate column composed of apex-sharing zinc–adeninate octahedral cages. The connection of zinc–adeninate columns and BPDC yield a 3D framework exhibiting a pcu network topology. By further modifying the reaction conditions, Rosi and coworkers obtained an exclusively mesoporous bio-MOF-100 (ref. 40) with a surface area of 4300 $m^2\ g^{-1}$ and the largest pore volume reported to date (4.3 $cm^3\ g^{-1}$).

2.2 Amine-functionalized MOFs with mixed linkers (MIXMOFs)

Amine-functionalized MOFs fabricated by mixed linkers were recently demonstrated based on the structures of MOF-5,[51] MIL-101 (ref. 52) and MIL-53.[53] In the case of amine-functionalized MIXMOFS, the molar ratios of amine-functionalized linkers and unfunctionalized linkers can be readily controlled by modifying the reaction stoichiometry. For example, a series of amine-functionalized MIXMIL-53 (ref. 53) with different amine contents were synthesized by replacing H_2BDC with NH_2BDC based on the synthesis conditions for pure MIL-53. Such amine-functionalized MIXMOFs were obtained by replacing the original organic linkers with amine-functionalized derivatives but without causing structural change. Herein, we refer these MIXMOFs as type 1. Moreover, some MIXMOFs were synthesised by two types of linkers exhibiting different geometries, such as DMOF-1-NH_2,[49] UMCM-1-NH_2 (ref. 49) and CPF-13.[50] We refer to them as type 2 MIXMOF. DOMOF-1-NH_2 was synthesized by the reaction between $Zn(NO_3)_2$ and the mixture of NH_2BDC and 1,4-diazabicyclo[2.2.2]octane organic linkers under solvothermal conditions. UMCM-1-NH_2 was fabricated by the mixed linkers of NH_2BDC and 4,4′,4″-benzene-1,3,5-triyl-tribenzoic acid and Zn nodes. The two amine-functionalized MIXMOFs are derivatives of previously reported structures, in which H_2BDC was replaced by NH_2BDC. CPF-13 (ref. 50) is an anionic porous amine-functionalized framework with amino-decorated polyhedral cages and is constructed from Zn ions, 3,5-diamino-1,2,4-triazole, and BDC linkers *via* solvothermal reactions. Interestingly, the BDC linker can be further replaced by NH_2BDC to fabricate frameworks but which exhibits low gas adsorption capacity because of the blockage of the pentagonal windows by the extra amino groups. To enlarge the framework windows, large 2,6-naphthalenedicarboxylic acid ligand was used by the authors to replace the BDC linker, however, resulting in an unstable structure.

2.3 Post-synthetic amine-functionalized MOFs

Amine-functionalized MOFs can also be prepared by PSM method. Hupp and coworkers[54] reported the covalent PSM of an alkyne functionalized MOF prepared from 2,6-naphthalenedicarboxylic acid and acetylene-tagged bis(pyridyl) mixed ligands. The alkyne group was initially protected by a silyl group during MOFs synthesis, and the protection was subsequently removed using tetrabutylammonium fluoride (TBAF). TBAF was chosen because the large size of the NBu^+ counterion can limit the deprotection to the surface of the MOF crystals. Furthermore, 'click' reaction was performed between the deprotected alkyne groups on the MOF crystal surface and dye ethidium bromide monoazide containing amino groups. Although the purpose of this work is not on the synthesis of amine-functionalised MOF, it offers a route to prepare amine-functionalized MOFs. Moreover, Stock and coworkers[55] successfully achieved a covalent PSM of MOF without active functional groups and obtained corresponding amine-functionalized MOFs. In particular, they selected MIL-101(Cr) for PSM because of its extraordinary chemical and thermal stability. They were able to directly functionalize the aromatic ring of the BDC ligand by nitric acid to produce MIL-101(Cr)-NO_2. The $-NO_2$ group was confirmed by IR spectroscopy and solution ^{1}H-NMR of MIL-101(Cr)-NO_2 upon digestion in

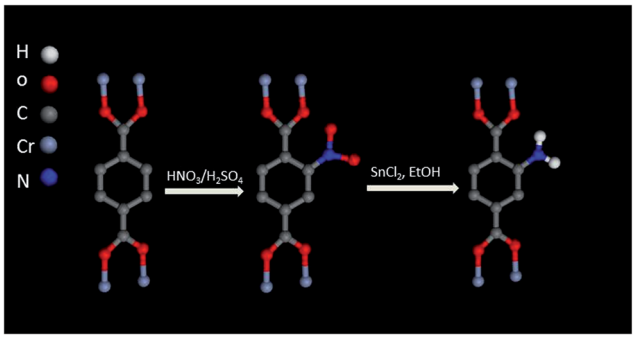

Fig. 3 Representation of the route for preparing NH_2-MIL-101(Cr) from MIL-101(Cr) *via* PSM.

aqueous NaOH. The $-NO_2$ groups in the MIL-101(Cr)-NO_2 can be easily and quantitatively reduced with $SnCl_2$ and EtOH into amino groups (Fig. 3).

Some MOFs, such as MIL-53 containing –OH groups, possess functional groups in their SBUs instead of in their organic linkers. In addition, several MOFs contain open metal sites in their SBUs after removal of coordinated solvent molecules. These traits render PSM of SBUs a mainstream approach for tuning the functionality of MOF pores. Herein, we will highlight several studies that successfully grafted amino groups onto SBUs. Ferey and co-workers[56] chose MIL-101(Cr), owing to its abundant unsaturated Cr sites, high surface area, and mesoporous pores, for PSM. In their study, MIL-101 was firstly heated under vacuum condition to remove the coordinated water molecules. Ethylenediamine (ED), which is an effective grafting reagent, was then chosen owing to its multifunctional chelating groups. ED was reacted with activated MIL-101 in toluene by heating under reflux and the products (ED-grafted MIL-101) were confirmed by PXRD and IR spectroscopy. In the resulting ED-grafted MIL-101 framework, the open metal sites of MIL-101(Cr) is anchored one end of ED, whereas the other amino end is left available (Fig. 4). A subsequent study also used ED for the PSM of a triazolate-bridged copper-based MOF (CuBTTri) following the procedure above.[57] In this MOF, the SBUs comprised chloride-centred $[Cu_4Cl]^{7+}$ squares, and each Cu centre possesses a coordinated solvent molecule. After removal of coordinated solvent molecules through heating, the MOF was exposed to a toluene solution of ED. The colour change in MOF crystals from red to blue in this process indicated successful grafting of ED. IR spectroscopy results and the reduced surface area further demonstrated that the ED ligands were successfully bound to the open Cu sites. A subsequent work further introduced *N*,*N*′-dimethylethylenediamine to the CuBTTri framework by using the same process.[58] The pore sizes of MOFs notably play an important role in the PSM for amine functionalization. For example, Mg-MOF-74 contains high concentration of open metal sites. However, amine-functionalized Mg-MOF-74 is difficult to achieve using PSM because its narrow pores limit the transport of reactants. Long and coworkers[59] recently exploited an expanded analogue of Mg-MOF-74, *i.e.* Mg_2(dobpdc), which exhibits 18.4 Å-wide channels. In the structure of Mg_2(dobpdc), each Zn^+ ion possesses four different $dobpdc^+$ ligands and one coordinated DEF solvent molecules, resulting in a distorted octahedral geometry. After activation, the MOF was suspended in hexane solution with an excess of *N*,*N*′-dimethylethylenediamine to prepare the alkylamine functionalized Mg_2(dobpdc). Lee and coworkers[60,61] very recently prepared heterodiamine-

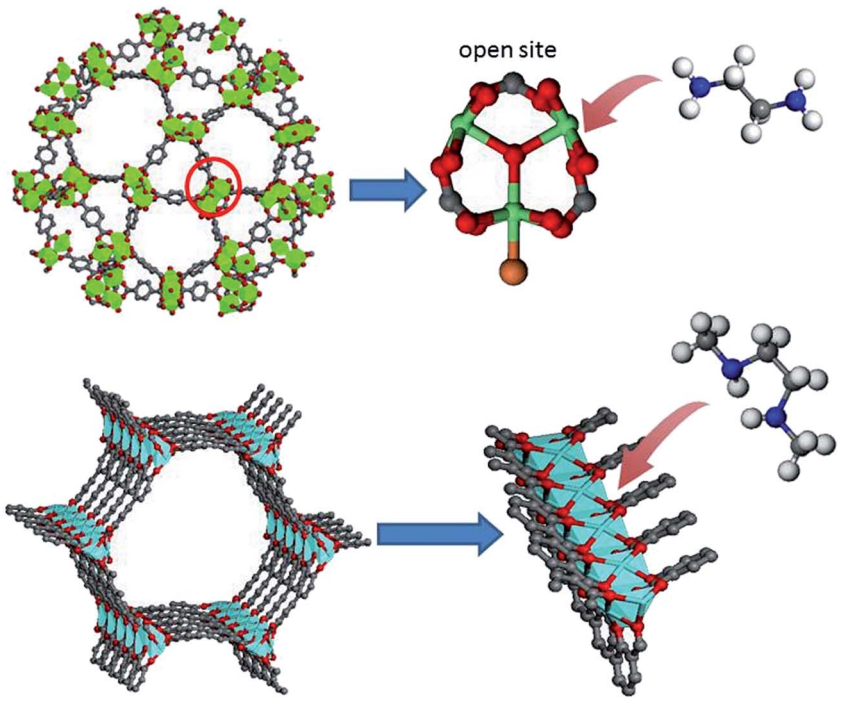

Fig. 4 Schematic route of grafting amines onto the open metal sites of MOFs. Top: MIL-101; bottom: Mg_2(dobpdc).

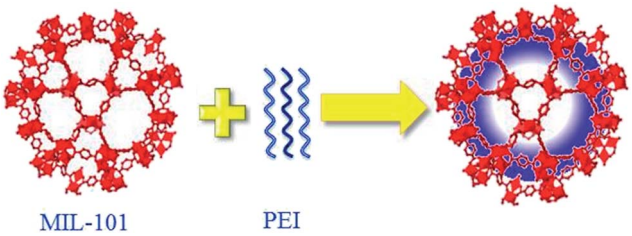

Fig. 5 Schematic of amine/MIL-101 composite preparation.

grafted Mg_2(dobpdc) and homodiamine-grafted Mg_2(dondc) by using the same route.

2.4 Physical incorporation of amine into MOFs

Physically incorporating amines into MOFs may be one of the most convenient methods to prepare amine-modified MOFs. Moreover, controlling the loading of amines is rather easy and much higher amine concentration can be achieved through this method compared with PSM. The amines to be incorporated should be polyamines because of the volatile nature of small amine molecules. However, the chain of polyamine should be short considering the relatively narrow pore windows of MOFs. The pore windows of candidate MOFs should be sufficiently large for polyamine impregnation. Pore windows with a diameter of several nanometres are preferred. For fast and facile polyamine impregnation, the MOF crystal should also be small. Chen *et al.*[62] have successfully prepared polyethylene (PEI)-impregnated MIL-101 (Fig. 5). During synthesis, activated MIL-101 was slowly added into a methanol solution of PEI under stirring. The resulting gel was stirred to dry under room temperature. MIL-101 was selected owing to its large surface area, as well as its excellent thermal and chemical stability. In addition, MIL-101 possesses open metal sites and Cr–OH groups that can serve as Lewis acid sites to anchor PEI. PEI impregnation was confirmed by IR spectroscopy, as well as by element and BET analyses. By using a similar process, Chen and coworkers further prepared PEI-modified NH_2-MIL-101(Cr)[63] composites and applied them in CO_2/CH_4 separation. The length of PEI used in the above is short with a molecular weight of 300. A subsequent study used several PEI with different molecular weights (ranging from 300 to 10 000) to detect the influences of PEI molecular weight on the performance of PEI-impregnated MIL-101(Cr).[64] The result shows that low-molecular-weight PEI-impregnated MIL-101(Cr) possesses high CO_2 capture capacity, indicating that low molecular-weight PEI with shorter length of PEI is beneficial for its diffusion into the MIL-101(Cr) pores. However, the main weakness of the NH_2-MIL-101 composite materials is its regeneration cost.

3. Applications of amine-functionalized MOF

MOFs have many applications owing to their high surface area and porosity, as well as versatile functionality. This section focuses only on the application of amine-functionalised MOFs by virtue of their amino functionality. We first discuss the application of CO_2 capture, which is the most extensively investigated in the last few years, then describe the amine-functionalized MOF-based membrane for gas separation and finally present their applications in catalysis.

3.1 CO_2 capture

Emission of CO_2 into the atmosphere is one of the major causes of global climate change. CO_2 capture in an efficient and economical manner is deemed a solution to mitigate CO_2 emission. MOFs are a promising candidate because they exhibit excellent CO_2 adsorption capacity at high pressures owing to their extremely high surface area. At high pressures, CO_2 adsorption capacities generally show a linear relationship with the specific surface area and pore volume of the adsorbents. However, most MOFs show unsatisfactory CO_2 adsorption capacities at low pressures (~0.15 bar), which are relevant to the realistic CO_2 emission conditions. For example, the CO_2 adsorption capacity of MIL-101(Cr) with large surface area and mesopores is 40 mmol g^{-1} at 50 bar.[65] However, at pressures below 1 bar, the CO_2 capture ability is unsatisfactory, due to the weak interaction between CO_2 and the frameworks. Although the imparted amino functionalities occupy the void space of MOFs and result in the decrease of surface area and pore volume, the abundant basic amino groups would still improve the CO_2 adsorption capacity of MOFs at low pressures. Clearly, the CO_2 capture ability at low pressures is mainly determined by the interaction between CO_2 molecules and active sties of MOFs. Chen and coworkers[20] recently developed amine-functionalized MIL-101, which exhibits higher CO_2 adsorption capacity at low pressures than that of MIL-101, although CO_2 adsorption capacity was low at high pressures owing to the decreased surface area.

Arstad and coworkers[18] investigated the CO_2 adsorption behaviours of three types of amine–MOFs and found that at low pressures, the MOF adsorbents with uncoordinated amine functionalities demonstrated higher CO_2 adsorption capacity than that of their unfunctionalized parents. Accordingly, enthalpy of CO_2 adsorption (50 kJ mol^{-1}) was much higher in the amine-functionalised MOFs than in the unfunctionalised parents.

$Zn_2(Atz)_2$ (ref. 35) exhibits high CO_2 adsorption capacity at low pressure and at 273 K (4.35 mmol g^{-1} at 1.2 bar), whereas no appreciable uptake of N_2, Ar and H_2 was observed under the same conditions. This selective CO_2 adsorption is partly attributed to the barrier of the small pores in the framework. However, this barrier can be overcome by host–guest interaction between CO_2 and amino groups. The adsorption enthalpy of CO_2 reaches 40.8 kJ mol^{-1} at zero coverage and the maximum loading is retained at 38.6 kJ mol^{-1}. To further understand the interaction between CO_2 and $Zn_2(Atz)_2$ frameworks, Shimizu and Woo[66] employed the single-crystal diffraction technique to locate CO_2 molecules within the structure. They found two independent CO_2 binding sites: one near the free amino groups (Fig. 6) and another one close to the oxalates. Their computational simulations indicated that three factors, including

appropriate pore size, amino groups and lateral binding between CO_2 molecules, are responsible for the large uptake of CO_2 in $Zn_2(Atz)_2$ at low pressures. Bio-MOF-11 (ref. 26) is another amine-functionalised MOF demonstrating excellent CO_2 adsorption capacity (up to 6.0 mmol g^{-1} at 1 bar and 273 K), high CO_2/N_2 selectivity (up to 81) and high heat of adsorption. Jiang *et al.*[67] conducted a molecular simulation study and found that Lewis basic amino and pyrimidine groups are the preferential adsorption sites. The high CO_2/N_2 selectivity of bio-MOF-11 is caused by the presence of multiple basic sites and by the nano-sized channels. These works demonstrate that, in addition to the Lewis basic amine sites, appropriate pore sizes play an important role for the high performance of amine-functionalized MOFs. CAU-1 exhibits pore windows of 0.3–0.4 nm, which is nearly similar to the dimensions of molecular CO_2. Thus, the combination of an appropriate pore size and amine groups render CAU-1 an ideal candidate for CO_2 capture. Si *et al.*[41] reported that CAU-1 demonstrates one of the highest CO_2 adsorption capacity (7.2 mmol g^{-1} at 273 K and 1 atm), high CO_2 adsorption heat (about 48 kJ mol^{-1} at the onset of adsorption) and excellent selectivity for CO_2 over N_2 and CH_4 at 1 bar (Fig. 7). The CO_2/N_2 and CO_2/CH_4 selectivity that were calculated based on the initial slopes[68] of CO_2, CH_4 and N_2 adsorption isotherms are 101 and 28, respectively. The highly selective adsorption of CO_2 over N_2 and CH_4 are further confirmed by breakthrough experiments (Fig. 7).

However, the covalent grafting of amine groups to the aromatic rings in MOFs cannot significantly enhance the affinity of CO_2 to amine groups resulting from the electron withdrawing property of benzene ring.[69,70] For example, the aforementioned NH_2-MIL-101(Cr) only shows slightly higher CO_2 adsorption capacity at low pressures than MIL-101(Cr). Couck *et al.*[27] found that the interaction of CO_2 in NH_2-MIL-53(Al) is stronger than that in MIL-53(Al) based on an *in situ* DRIFTS analysis. The presence of amine groups in MIL-53(Al) was initially attributed to the enhanced affinity of CO_2. However, a follow-up work[69] demonstrated that the role of the amine groups is only indirect, and the enhanced CO_2 adsorption and separation ability of NH_2-MIL-53(Al) are mainly attributed to the specific flexibility of framework.

Incorporation of alkylamines which have higher affinity to CO_2 molecules into MOF pores is expected to improve the capacity of MOFs for CO_2 uptake at low partial pressures. A pioneering work showed that ED-modified CuBTTri (en-CuBTTri)[57] was successfully prepared and demonstrated a record for isosteric heat of CO_2 adsorption, *i.e.* 90 kJ mol^{-1} at zero coverage. However, only a slightly enhanced CO_2 uptake was achieved, probably caused by the clogging of the outermost framework pores, thereby limiting the loading amount of ED. Motivated by this work, the authors further developed mmen-CuBTTri[58] with high loading of *N*,*N*′-dimethylenediamine, resulting in an adsorbent demonstrating exceptional CO_2 capture ability (Fig. 8). Although the surface area of CuBTTri decreased after attachment of *N*,*N*′-dimethylenediamine to the open metal sites, CuBTTri displayed a drastically enhanced CO_2 adsorption capacity. At 25 °C and 0.15 bar, mmen-CuBTTri can capture 2.38 mmol g^{-1} and shows an excellent CO_2/N_2 selectivity of 327 based on the ideal adsorbed solution theory (IAST) under a designed gas mixture of 0.15 bar CO_2 and 0.75 bar N_2. This high capacity and selectivity were ascribed to the exceptionally large isosteric heat of CO_2 adsorption (−96 kJ mol^{-1}) at zero coverage, which was attributed to the chemisorption between CO_2 and amines as revealed by the infrared spectra analysis. Importantly, mmen-CuBTTri can be regenerated at 60 °C despite the large initial heat of adsorption. After 72 adsorption/desorption cycles, mmen-CuBTTri showed no loss in CO_2 adsorption capacity. Another study attempted to search for a material showing an improved performance for CO_2 capture from the atmosphere and dry flue gas. The *N*,*N*′-dimethylenediamine-modified Mg_2(dobpdc)[59] was then developed as a remarkable new CO_2 adsorbent exhibiting large capacity, high selectivity and rapid kinetics for CO_2 adsorption from dry gas mixture with N_2 and O_2. At 25 °C and 0.39 mbar atmospheric pressure of CO_2, the alkylamine-functionalised MOF possesses a CO_2 adsorption capacity of 2.0 mmol g^{-1}, which is 15 times that of the parent MOF. At a pressure of 5 mbar, which is the partial pressure of CO_2 in the International Space Station, the value reaches to 2.6 mmol g^{-1} (10.3 wt%), which is much larger than that of zeolite 5A which is currently used in the station. In addition, the calculated isosteric heat of adsorption for CO_2 reaches a value of −71 kJ mol^{-1}, which likely corresponds to the chemical adsorption of CO_2 onto the free amine of *N*,*N*′-dimethylenediamine. The *in situ* diffuse reflectance infrared Fourier transform spectroscopy technique was employed to confirm the chemical adsorption characteristics. Surprisingly, the selectivity of alkylamine-functionalized MOF for CO_2 over N_2 in air was at least 49 000. At 0.15 bar and 40 °C, which are conditions relevant to CO_2 capture from flue gas, the *N*,*N*′-dimethylenediamine-modified Mg_2(dobpdc) takes up 3.14 mmol g^{-1} of CO_2 molecules. The cyclic CO_2 adsorption/desorption property of alkylamine-functionalized was further evaluated using thermogravimetric analysis under dynamic environments.

Compared with grafting amines to MOFs *via* chemical interaction, physical impregnation of poly-alkylamines into MOFs will render more active amine groups and maintain the strong interaction between CO_2 and alkylamine groups. Chen and coworkers[62] recently reported PEI-incorporated MIL-101 composite for CO_2 capture. A series of PEI-incorporated MIL-

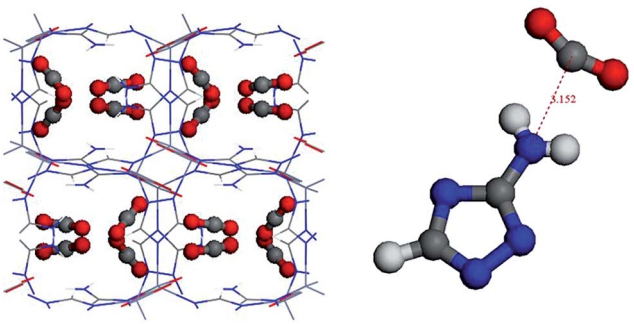

Fig. 6 Locations of CO_2 adsorbed in the $Zn_2(Atz)_2$. Ball: blue, N; white, H; gray, C.

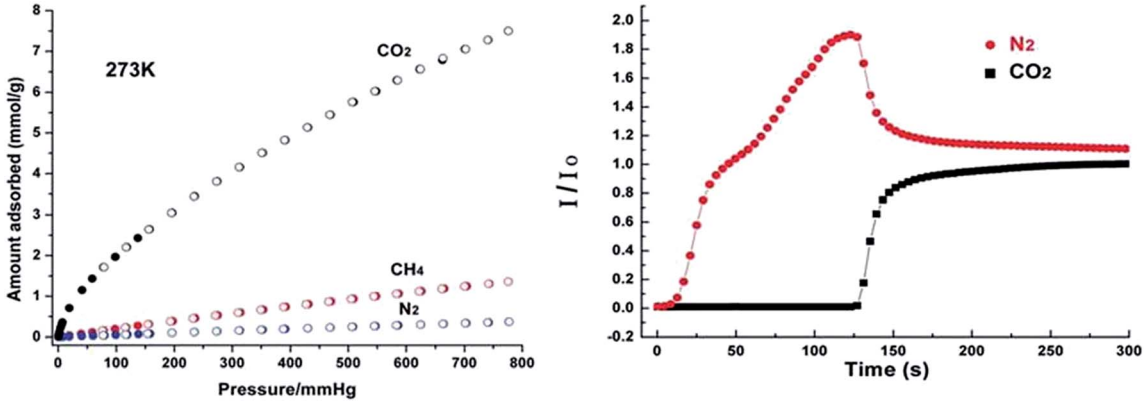

Fig. 7 (Left) Adsorption isotherms for CO_2, N_2 and CH_4 at 273 K. (Right) Breakthrough experiment of an equimolar CO_2/N_2 mixture at 0.1 MPa and 273 K. Reprinted from ref. 41 with permission from Royal Society of Chemistry.

101(Cr) adsorbents with different PEI loadings were prepared *via* a simple impregnation process. All of the resulting composites exhibit dramatically enhanced CO_2 adsorption capacity at low pressures, although the surface area and pore volume of MIL-101(Cr) are significantly decreased (Fig. 9). Among them, the MIL-101 loaded with 100 wt% PEI (PEI-MIL-101-100) displays a CO_2 adsorption capacity of 4.2 mmol g^{-1} at 25 °C and 0.15 bar. This value is much higher than that of 30% MEA solution[71] and PEI-incorporated zeolites.[72] PEI-MIL-101 materials also show excellent moisture stability. More importantly, the PEI-modified MIL-101 displays rapid adsorption kinetics and ultrahigh selectivity for CO_2 over N_2 in the design flue gas with 0.15 bar CO_2 and 0.75 bar N_2. For example, the PEI-MIL-101-100 possesses a CO_2/N_2 selectivity of up to 770 at 25 °C, and the CO_2 adsorption capacity in PEI-MIL-101-100 can reach 98% of its saturation within the first 5 min. After five adsorption/desorption cycles, no reduction in CO_2 capacity was observed in the PEI-MIL-101-100. A subsequent work found that the PEI-modified NH_2-MIL-101 (ref. 61) exhibits ultrahigh CO_2/CH_4 selectivity.

Furthermore, working capacity[70,73] is one of the most important factor in evaluating the capacity of an adsorbent to capture CO_2 from flue gas streams. In pressure swing adsorption, this parameter is calculated as the difference between the quantity adsorbed at flue gas and the quantity adsorbed at low purge pressure. In temperature swing adsorption, this parameter is evaluated by taking the difference between the quantity adsorbed at flue gas condition and the quantity adsorbed at desorbed temperature (Fig. 10). Given the good affinity between CO_2 and amine-functionalized MOFs, the pressure swing methods is not suitable to regenerate the amine-functionalized MOFs. However, for temperature swing methods, the amine-functionalized MOFs[58,59] with high heats of adsorption (high affinity) are better candidates than the MOFs with moderate or low heats of adsorption. Long[73] *et al.* described the scheme of temperature swing adsorption. In their study, the working capacity of mmen-CuBTTri is nearly 7 wt% as measured by thermogravimetric analysis upon mixing 15% CO_2 with N_2 at 25 °C with a desorbed temperature of 60 °C. This working capacity is greater than that of 30% MEA solution, which is frequently

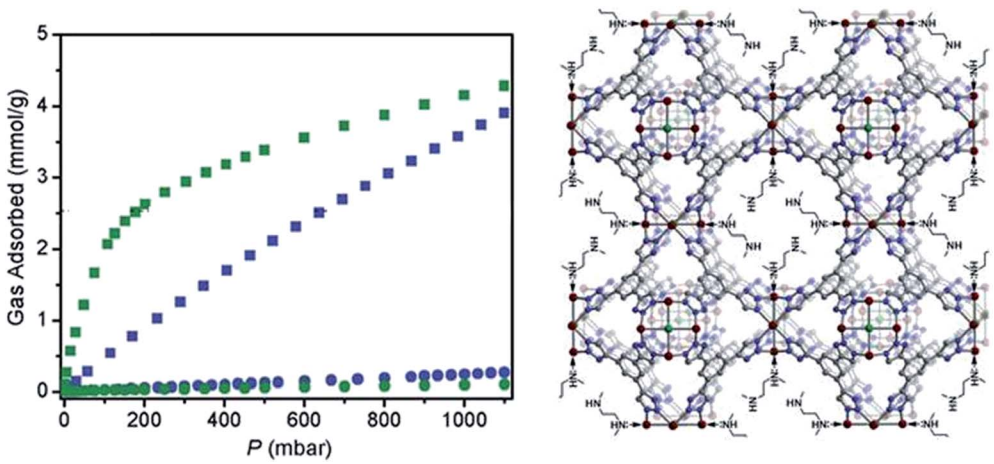

Fig. 8 Isotherms for CO_2 (squares) and N_2 (circles) adsorption at 25 °C for mmen-CuBTTri (green) and CuBTTri (blue). Reprinted from ref. 58 with permission from Royal Society of Chemistry.

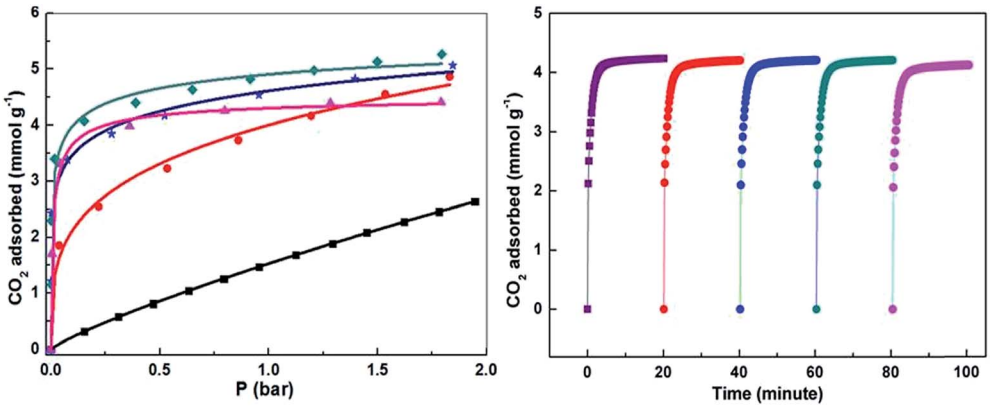

Fig. 9 (Left) CO_2 adsorption isotherms of MIL-101(Cr) before and after PEI loading at 25 °C. Symbol: ■ MIL-101, ● PEI-MIL-101-50, ★ PEI-MIL-101-75, ◆ PEI-MIL-101-100 and ▲ PEI-MIL-101-125. (Right) Cycling CO_2 adsorption kinetics of PEI-MIL-101-100. Reproduced from ref. 62 with permission of Nature Publishing Group.

reported to be 5.5 wt%. For mmen-Mg_2(dobpdc), a working capacity of 7.2 wt% was realized when 15% CO_2 in N_2 at 40 °C was desorbed with 100% CO_2 at 150 °C. Lee and coworkers[60,61] further prepared *N*,*N*′-dimethylethylenediamine (dmen)-modified Mg_2(dobpdc) and obtained an elevated working capacity (11.7–13.5 wt%).

The working capacity can also be evaluated from single component gas adsorption isotherms (Fig. 10 left), which are somewhat lower than that measured by thermogravimetric analysis. Points C and A are the amount adsorbed at 0.15 bar and 40 °C and at 1 bar and 150 °C, respectively. The working capacity was thus calculated as the difference between points A and C.

For classification and comparison, we summarized the CO_2 uptake of amine-functionalized MOFs in Table 2. We can draw some conclusions on the basis of these works, and these conclusions are useful in developing excellent CO_2-absorbing materials: (i) in the case of pure amine-functionalized MOFs, appropriate pore sizes and active amine groups were both investigated. (ii) In alkylamine-appended MOFs prepared *via* by post modification, the pore size of MOFs should be sufficiently large for the transport of alkylamine; moreover, active sites, such as open metal sites, are also required. (iii) To achieve polyamine-based MOF exhibiting excellent performance, the pore windows and pore volume of the MOF should be sufficiently large for polyamine impregnation and loading.

3.2 Membranes for gas separation

Owing to their high energy efficiency, low cost and ease of processing, membranes with gas separation ability have attracted much attention in the last decades. MOF membranes are the latest and most exciting material for gas separation owing to their well-defined, highly regular pore size and tunable functionalities. Although some MOF membranes have been fabricated and tested for gas separation, research on this subject is still in its infancy. Herein, we will focus on the research progress in gas separation using pure amine-functionalized MOF membranes and mixed matrix membrane (MMM) containing amine-functionalized MOF nanoparticles.

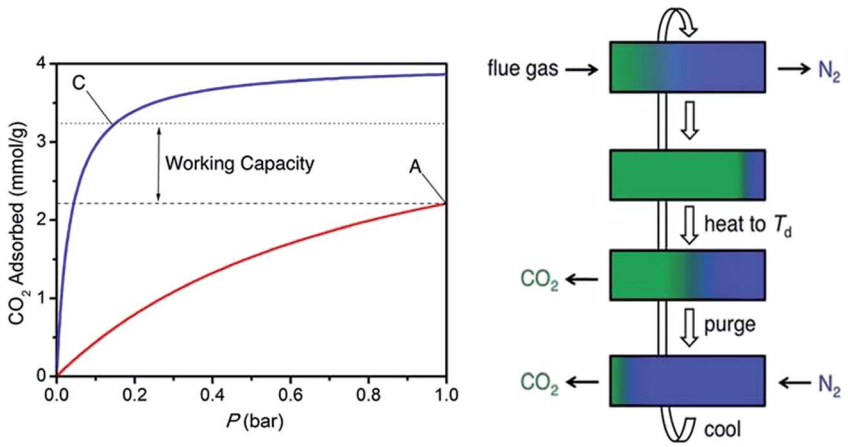

Fig. 10 (Left) CO_2 adsorption isotherms at 40 °C and 150 °C. Reprinted from ref. 59. Copyright 2012 American Chemical Society. (Right) Schematic representations of temperature swing adsorption. Reprinted from ref. 73 with permission from Royal Society of Chemistry.

Table 2 CO_2 adsorption capacity of amine-functionalized MOFs

	CO_2 uptake at 273 K (mmol g^{-1})		CO_2 uptake at 298 K (mmol g^{-1})			
Acronym name	0.15 bar	1 bar	0.15 bar	1 bar	Q_{st} (zero coverage)	Ref.
CAU-1	—	7.2	—	3.9	48	41
NH_2-MIL-53, (USO-1-Al-A)	—	~1.5	—	~1.1	~56	74
	—	—	—	~3.0	50	18
NH_2-MIL-101(Cr)	—	3.2	—	1.9	~52	20
en-CuBTTri	—	—	0.366 (0.06 bar)	—	~90	57
mmen-CuBTTri	—	—	2.38	4.2	96	58
$Zn_2(CN_5H_2)_3(H_2O)_3$	—	2.4	—	—	—	37
mmen-Mg_2(dobpdc)	—	—	3.13	3.86	~75	59
Bi-MOF-11	—	6.0	—	4.1	~45	38
$Zn(Atz)_2$	—	4.35 (1.2 bar)	—	—	~40.8	35
CPF-13	—	5.2	—	3.62	~28.2	50
PEI-MIL-101-100	—	—	4.2	5.0	—	62
Uio-66-NH_2	—	—	1.1	—	28	56
NH_2-MIL-125	—	3.0	—	—	—	23
MAF-66	—	6.26	—	4.41	26	34
IRMOF-74-III-$CHNH_2$	—	—	—	3.2	—	75
dmen-Mg_2(dobpdc)	—	—	3.77	—	—	60
mmen-Mg_2(dondc)	—	—	4.13	—	—	61

3.2.1 Pure amine-functionalized MOF membranes. Nano seeds are usually required for MOF membrane growth. However, in most cases, MOFs are obtained as single crystals with a size of up to several millimetres or microcrystals. Synthesizing nano-sized MOFs for membrane fabrication is considerably difficult. For example, no nano IRMOF-3 crystals have been prepared to date. Therefore, we cannot obtain high-quality IRMOF-3 membrane using the conventional methods. To address this problem, Jeong and Yoo[76] developed a route using IRMOF-1 nanocrystals as seeds for IRMOF-3 growth. The IRMOF-1 nano crystals were prepared under microwave as reported. Unfortunately, the obtained activated IRMOF-3 layer was a film and not a membrane on the basis of the substantial amount of cracks in or between the IRMOF-3 crystals. To address this problem, surfactants were used as additives during activation of the IRMOF-3 membrane (Fig. 11); finally, a crack-free IRMOF-3 membrane was successfully prepared.[77] The resulting IRMOF-3 membrane showed a preferential H_2 permeation with a Knudsen-type transport similar to that of IRMOF-1. Interestingly, the permeance of CO_2 through the IRMOF-3 membrane was much higher than the predicted Knudsen permeance. This finding can be ascribed to the strong interaction between CO_2 and amino groups of IRMOF-3. However, the selectivity of the resulting IRMOF-3 membrane are very low, even less than the Knudsen separation factors.

NH_2-MIL-53 is a well-known MOF owing to its breathing effect and amine functionality. Motivated by the gas adsorption properties of NH_2-MIL-53, Zhu and coworkers[74] produced a thin NH_2-MIL-53 membrane for H_2 separation *via* the route involving colloidal assembly of MOF seeds. The resulting membrane is crack-free and approximately 15 μm thick. Single gas permeation test indicated a decreasing permeance in the following order: $H_2 > CH_4 > N_2 > CO_2$. The calculated ideal selectivity of H_2 over CH_4, N_2 and CO_2 are 18.5, 19.5 and 27.3, respectively, which are much larger than the corresponding Knudsen separation factors and nearly similar to the highest reported values.[78,79] Interestingly, the pore size of NH_2-MIL-53(Al) was far beyond the size gas molecules, indicating that molecular sieving cannot explain this phenomenon. Therefore, the authors attributed it to the difference of gases intrinsic diffusion properties combined with the effect of adsorption. At elevated temperatures, the permeances of all the test gases increases, whereas the H_2 permselectivities over other gases decreases. Nevertheless, the permselectivities of H_2 over CH_4,

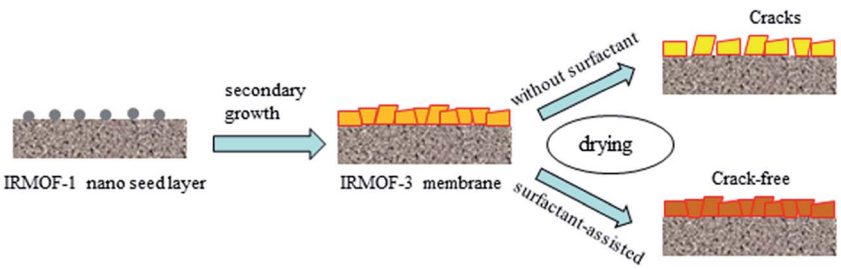

Fig. 11 Schematic representation of the fabrication of crack-free IRMOF-3 membranes using the surfactant-assisted drying method.

N_2 and CO_2 at 353 K are 9, 12 and 17, respectively, which were still much higher than their Knudsen separation factors. Furthermore, the performance of NH_2-MIL-53(Al) membrane in gas mixtures was evaluated. The results showed that the membrane possesses high efficiency of hydrogen separation from the gas mixtures at equal volume ratio of H_2/CH_4, H_2/N_2 and H_2/CO_2. The H_2 permeance of the NH_2-MIL-53 membrane measured in the gas mixtures is higher than that of ZIF-90,[78] ZIF-22 (ref. 79) and ZIF-8.[80] Moreover, the H_2 separation factors in H_2/CH_4, H_2/N_2 and H_2/CO_2 reach up to 23.9, 30.9, and 20.7 respectively. The thermal stability of NH_2-MIL-53 membrane was further evaluated and the results have proven that the membrane possesses good reversibility upon temperature cycling (288–353 K), as well as high thermal stability. Chen *et al.*[81] also fabricated NH_2-MIL-53(Al) membrane using a different method and then tested for gas separation. NH_2-MIL-53(Al) crystals can be prepared using DMF or water as solvent. However, the corresponding resulting crystal morphologies and sizes vary.[27,82] Zhu *et al.* used DMF solvent for membrane fabrication, whereas Chen *et al.* used water as solvent. Interestingly, the NH_2-MIL-53(Al) membrane prepared by Chen *et al.* shows much lower H_2 selectivity (only approximately 4.5 for H_2/CO_2) but displays had a much higher H_2 permeance (1.5×10^{-5} mol m^{-2} Pa^{-1} s^{-1} at room temperature) than that obtained by Zhu *et al.*

CAU-1 is another amine-functionalised MOF that was successfully synthesised as a membrane supported on asymmetric α-Al_2O_3 tube. Zhu *et al.*[83] reported the first CAU-1 membrane, which was applied in hydrogen purification. The CAU-1 membrane was fabricated by secondary growth with CAU-1 nanocrystals seeds. During membrane fabrication, the α-Al_2O_3 tube was not only the support; aluminium also provided additional support. The CAU-1 membrane exhibits preferential permeation for H_2 with ideal separation factors of 13.27 for H_2/CO_2, 9.6 for H_2/N_2 and 10.84 for H_2/CH_4. The calculated separation factors and gas permeances for binary gases mixtures are similar to the results of single gas test. Yang and coworkers[86] recently synthesised a high-quality CAU-1 membrane using a similar procedure but with a different activation process. This CAU-1 membrane showed very excellent CO_2/N_2 selectivity with an ideal separation factor of up to 26.2 at room temperature (Fig. 12). The separation performance of the membrane was further tested using CO_2 and N_2 mixtures at room temperature. When the CO_2 mole fraction in the feed steam was increased from 0.1 to 0.9, the corresponding CO_2/N_2 separation factors ranging from 17.4 to 22.8 were obtained. Interestingly, this CAU-1 membrane demonstrates the highest CO_2 permeance at 1.32×10^{-5} mol m^{-2} Pa^{-1} s^{-1} at room temperature; this value more than twice larger that for hydrogen. This result was obviously opposite to that of Zhu in which the H_2 displays the highest permeance, whereas CO_2 exhibits the lowest permeance. Yang and his coworkers speculated that the different result obtained by Zhu was caused by the problem on the activation of their membrane. Nevertheless, the result is slightly surprising, and this topic must be further investigated.

Wang and coworkers[84] recently fabricated an amine-functionalized Mg-MOF-74 membrane *via* PSM. They have first grown a Mg-MOF-74 membrane on the surface of alumina substrate with MgO as the seeds, and then modified the membrane with ED to obtain ED-grafted Mg-MOF-74. They found that the separation performance of the amine-functionalized Mg-MOF-74 membrane is much better than that of the original Mg-MOF-74 membrane, and the H_2/CO_2 selectivity reaches up to 28 compared the original value of 10.5.

Fabricating amine-functionalized MOF membranes for CO_2/CH_4 separation is also very promising and is of great interest from both the environmental and energy perspective owing to the preferential CO_2 adsorption property of amine-functionalized MOF. As a candidate, bio-MOF-1 was assembled as a membrane and tested for CO_2/CH_4 separation by Carreon and Bohrman.[85] The bio-MOF-1 membrane was prepared *via* secondary seeded growth in tubular porous stainless steel supports. The quality of the resulting membrane was demonstrated by XRD analysis and SEM. A CO_2/CH_4 selectivity of 2.6 and a permeance of 11.9×10^{-5} mol m^{-2} Pa^{-1} s^{-1} were achieved for the bio-MOF-1 membrane. The authors proposed that the selective transport pathway for CO_2 is mainly attributed to the presence of adeninate amino basic sites in the

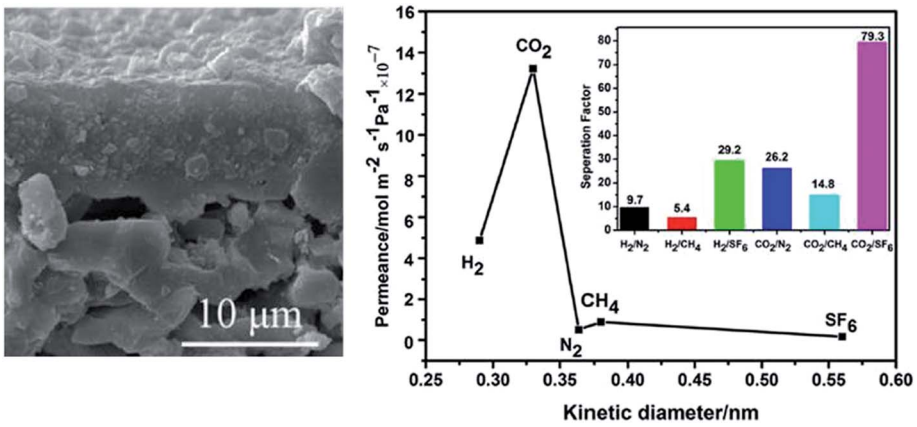

Fig. 12 CAU-1 membrane SEM image and single gas permeances at room temperature. Reprinted from ref. 84 with permission from Royal Society of Chemistry.

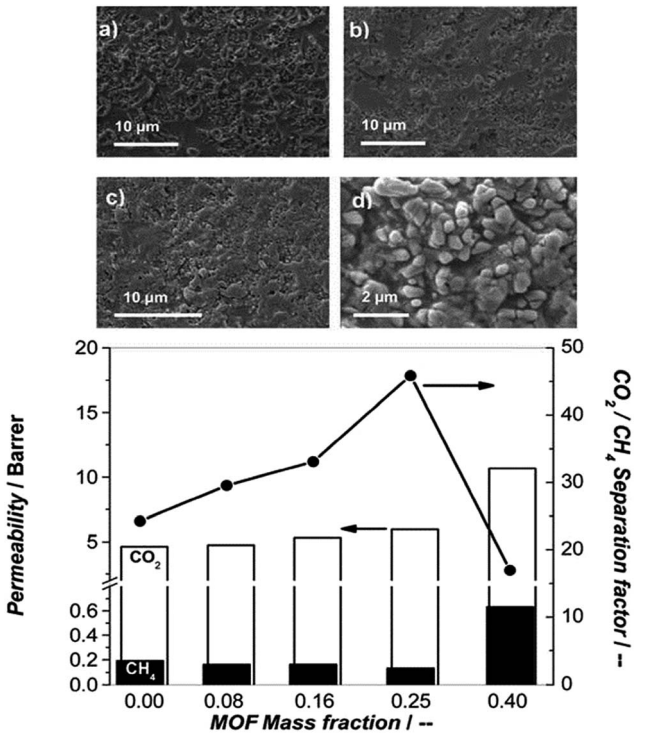

Fig. 13 SEM micrographs of the cross section of mixed matrix membrane containing 8 (a), 16 (b), 25 (c) and 40 (d) wt% NH_2-MIL-53(Al) crystals. Reprinted from ref. 92 with permission from Royal Society of Chemistry.

pores. In addition, another amine-functionalized MOF in bio-MOFs series, bio-MOF-11 membrane were predicted by molecular simulation to possess CO_2/CH_4 selectivity of ~5.[87]

3.2.2 Mixed matrix membrane. MMMs, which exhibit high separation properties and permeance, have emerged in the last few decades as potential candidates for industrial applications.[88] MMMs are prepared by incorporating inorganic fillers into various polymers. Although some successes have been achieved through this approach, the resulting MMMs often exhibit void spaces between the filler and the polymeric matrix, resulting in a loss of selectivity compared with the parent polymer. Incorporation of MOF nanoparticles into a polymer matrix has recently attracted much attention owing to the various properties of these nanoparticles, which can potentially create a breakthrough in the field of gas separation. Although some MOF-based MMMs[89–91] have been reported in the last few years, the subject is still in its infancy. Among the great amount of MOFs, the amine-functionalized MOFs offer at least the following advantages: (i) their excellent selective gas adsorption properties and (ii) the interaction between amino groups and polymer matrix that facilitates matching between MOF and polymer matrix. Therefore, the amine-functionalized MOF-based MMMs are highly anticipated to display high performance for gas separation.

Kapteijn *et al.*[92] used NH_2-MIL-53(Al) as an MMM filler for PSF polymer. A series of NH_2-MIL-53(Al) MMMs with different NH_2-MIL-53(Al) loading was successfully fabricated (Fig. 13). SEM characterisation of the MMMs confirmed the excellent MOF–polymer matching even at 40 wt% loading. Authors attributed this finding to hydrogen bonding between the amino groups of NH_2-MIL-53(Al) and sulfone groups of PSF. Gas permeation tests revealed the best performing membrane (25 wt% loading) demonstrating a moderate CO_2 flow and the highest CO_2/CH_4 selectivity (~45). In a following work, Rodrigue and his coworkers[47] fabricated another NH_2-MIL-53(Al)-based MMM using 6FDA-ODA-based polyimides as polymer matrix, and found that MOF-polyamine with 30 or 32 wt% content of NH_2-MIL-53(Al) yields data points above the Robeson's upper bound-1991.[93]

Kaliaguine *et al.*[94] prepared UiO-66-NH_2 and NH_2-CuBTC (with 25% ABDC and 75% BDC)-based MMM using 6FDA-ODA polyamine as polymer matrix and 25 wt% MOF particles as fillers. The cross-sectional SEM image confirmed the good affinity between the UiO-66-NH_2 and bulk polymer resulting from hydrogen bonding between the amine groups and the carboxylic acid groups in the polymer. However, this good affinity renders the polymer rigid at the interface and thus slightly decreases the permeability. Nevertheless, 6FDA-ODA/UiO-66-NH_2 shows enhanced CO_2/CH_4 selectivity (by 17%) compared with the neat polymeric membrane. In the case of 6FDA/NH_2-CuBTC, both the permeability and selectivity are greatly enhanced. The elevated CO_2 permeability was speculated to have been caused by the presence of the whiskers and by increased roughness on the NH_2-CuBTC crystal surface. In addition, data for both 6FDA-ODA/UiO-66-NH_2 and 6FDA-ODA/NH_2-CuBTC lie on the Robeson upper bound-1991.

Chen *et al.*[95] recently fabricated the first CAU-1-based MMM that demonstrates high H_2 permeance and H_2/CO_2 selectivity by using poly(methyl methacrylate) (PMMA) as matrix (Fig. 14). The high-performance MMM was attributed to the good dispersion of CAU-1 and to excellent interfacial contact with the PMMA resulting from the considerable amount of hydrogen bonds. By optimising the loading of CAU-1 particles, a H_2/CO_2 selectivity of up to 13 and a high H_2 permeance of 1.1×10^4 barrer were achieved. The permeability of H_2 achieved herein is three orders of magnitude higher than those of reported MMMs. The synergetic effects of the thin PMMA membrane and the incorporated CAU-1 particles are believed to have made major contribution to the high performance of the MMM for H_2/CO_2 separation.

3.3 Catalysis

Solid basic catalysts are highly required in sustainable chemistry owing to their higher efficiency in reactions and higher turnover number compared with strong soluble bases. In addition, the use of solid catalysts simplifies the processes and significantly reduces the volume of waste. However, leaching of active sites/material from solid catalysts limits the progress in this area. MOFs with non-coordinated amino groups, such as IRMOF-3 and NH_2-MIL-53, are potential candidates for this application.

The amino groups of IRMOF-3 interacts very readily with different solvents.[96] In addition, an intramolecular hydrogen bonding between amino groups and a carboxylate oxygen atom

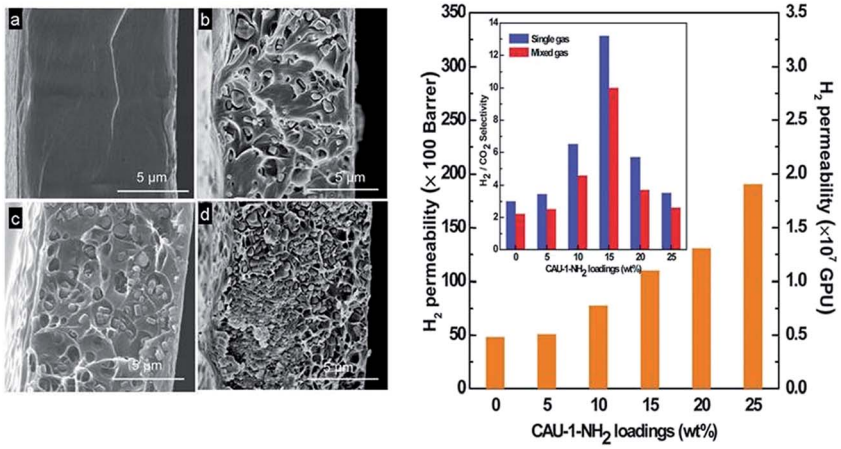

Fig. 14 Left: SEM images of the cross section of pure poly(methyl methacrylate) membrane (a) and MMMs with 5 wt% (b), 15 wt% (c) and 25 wt% (d) CAU-1 loading. Right: H_2 permeability of the MMMs with different CAU-1 loadings and the corresponding H_2/CO_2 selectivities (inset). Reprinted from ref. 95 with permission from Royal Society of Chemistry.

forms within the IRMOF-3 framework. The electron-donating oxygen from the carboxylic group may also increase the basic strength of IRMOF-3. Kapteijn *et al.*[97] have investigated the catalytic activity of IRMOF-3 as a solid basic catalyst in Knoevenagel condensation of ethyl cyanoacetate and ethyl acetotacetate with benzaldehyde. Three types of IRMOF-3 crystals with different surface areas were prepared. The result revealed the activity of IRMOF-3 depends on a specific surface area. IRMOF-13_{DEF} (synthesised with DEF solvent) with the largest surface area exhibits the best activities with a 100% selectivity in Knoevenagel condensation of ethyl cyanoacetate and ethyl acetotacetate with benzaldehyde (Fig. 15). The catalytic activity correlated with the surface area of IRMOF-3 was ascribed to the different accessibility of the active amino groups. Importantly, the diffusion limitations were absent in IRMOF-3 catalyst, which is stable under the studied conditions and can be reused without significant loss of activity. Another amine-based MOF, NH_2-MIL-53(Al) was also studied for condensation. The results showed that NH_2-MIL-53(Al) possessed poor performance during condensations, and this result is attributed to the strong adsorption and diffusion limitations in the 1D pore structure of the framework with breathing effects. In addition, the performance of IRMOF-3 catalyst during condensation in different solvents was also investigated, and the catalyst displays a homogenous behaviour.

Furthermore, Gascon and Kapteijn[31] reported the activity of NH_2-MIL-101(Al) in the same reaction. The performance of NH_2-MIL-101(Al) in the Knoevenagel condensation of benzaldehyde and ethyl cyanoacetate was better than that of IRMOF-3 and NH_2-MIL-53(Al). Interestingly, the activity of NH_2-MIL-101(Al) in apolar solvent is much higher than that of in apolar solvent, while the activity of IRMOF-3 in apolar is greatly suppressed. The authors provided a possible explanation for this finding: the amines of the supertetrahedra of the NH_2-MIL-101(Al) framework possibly exhibit a higher basicity than those of amines at the windows of the cages of NH_2-MIL-101(Al); this higher basicity is caused by NH_2–H_2N and NH_2–OH hydrogen bonding interactions. Hartmann *et al.*[44] further synthesized a NH_2-MIL-101(Al) with high specific pore volume (1.53 $cm^3\ g^{-1}$) and surface area (3099 $m^2\ g^{-1}$) using an improved synthesis protocol. They tested NH_2-MIL-101(Al) in Knoevenagel condensation of benzaldehyde with malononitrile and with ethyl cyanoacetate. For comparison, NH_2-MIL-101(Fe) and CAU-1 were also tested. NH_2-MIL-101(Al) and NH_2-MIL-101(Fe) are both excellent catalysts in the reaction of benzaldehyde with malononitrile, and approximately 90% yield of benzylidene malononitrile was obtained after 3 h. No appreciable difference in activity of NH_2-MIL-101(Al) and NH_2-MIL-101(Fe) was observed in the reaction of benzaldehyde with ethyl cyanoacetate, indicating that the metal ions in the framework play only a minor role. Only CAU-1 exhibited poor activity under the same conditions, which can be attributed to the much smaller pore windows of CAU-1 (0.3–0.4 nm) compared with that of MIL-101 structure (~1.6 nm). In addition, mesoporous UMCM-1-NH_2 with higher catalytic activities than those of IRMOF-3 was further reported.[98]

Farrusseng *et al.*[99] investigated the solvent-free base catalysis and transesterification based on amino-functionalized MOFs,

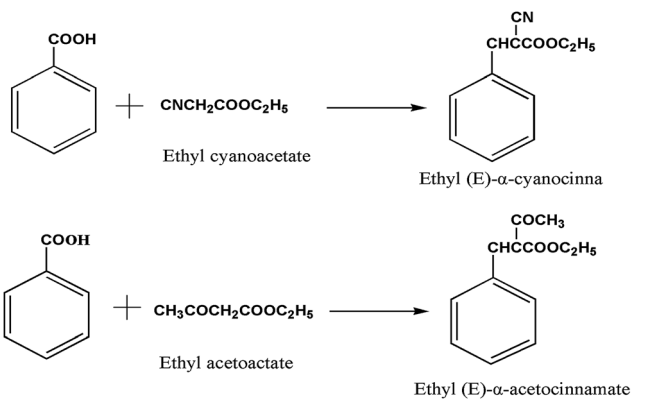

Fig. 15 Knoevenagel condensation of benzaldehyde with ethyl cyanoacetate and ethyl acetoacetate.

and they chose two amine-functionalized MOFs, namely, IRMOF-3 and ZnF(Am_2TAZ). To increase the hydrophobicity and maintain a similar level of basicity, the two amine-functionalised MOFs were post-functionalized with pyridine groups, producing IRMOF-3-pyridine and ZnF(Am_2TAZ)-pyridine, which were confirmed by ^{1}H NMR and mass spectrometry analysis. This work used aza-Michael reaction as the model reaction to evaluate the base catalysts because. For comparison, alkylamino-functionalized mesoporous ordered silica MCM-41 and its post-functionalized compound were prepared and tested. The experimental results indicated that the functionalized MOFs exhibited superior yields with regard to functionalized MCM-41 materials. In addition, the post-functionalized MOFs exhibited slightly higher activity than their parents. In the case of ethyldecanoate transesterification with MeOH, all of the MOFs demonstrated up to 95% conversion after 24 h at 180 °C. Moreover, IRMOF-3 and IRMOF-3-pyridine exhibit the highest catalytic activities at a lower temperature. The MOF catalysts can also be reused twice without showing loss of activity. Baiker *et al.*[100] reported the catalysis behaviour of a MIXMOF ($Zn_4O(BDC)_x(ABDC)_{3-x}$) isostructural to MOF-5 in the reaction between propylene oxide and carbon dioxide. The authors found that the activity of MIXMOF depends on the number of amino groups. Under optimized reaction conditions, the MIXMOF with 40% ABDC displays a high activity with a propylene carbonate yield of 63%.

ED-grafted ED-MIL-101,[56,101] which is an amine-functionalized MOF derived though PSM, is also an excellent catalyst in Knoevenagel condensation. With a small amount of ED-MIL-101, the conversion of the condensation of benzaldehyde with cyanoethyl acetate reaches up to 97.7% at 353 K for 19 h and with a high selectivity of 99.1%. The catalytic activity of ED-MIL-101 is much better than that of APS-SBA-15 (conv. 74.8%, sel. 93.5%), which contains more free amine groups. In addition, the amine-functionalized MOF allows PSM one to achieve a desired functionality for catalysis. For example, Cohen *et al.*[102] reported a postsynthetic NH_2-MIL-53(Al) and a MIL-53-AMMal with Bronsted acid catalytic sites.

4. Conclusions

As shown by the above literature reports, amine-functionalized MOFs have become a topic of central importance to the MOFs family. Many studies on amine-functionalized MOFs are flourishing with exciting new findings in the areas of CO_2 capture, gas separation, catalysis and simply the discovery of new materials and structure types. Currently, one of the main challenges is the syntheses of amine-functionalized MOFs due to the thermally labile functional groups of ligands. Apart from the most widely used *in situ* synthesis methods, the PSM and physical impregnation techniques are emerging and shown to be very useful. They have demonstrated to be applicable for some compounds, such as mmen-Mg_2(dobpdc) and PEI-MIL-101(Cr), under mild conditions. This could be of great interest for preparing amine-functionalized MOFs with high amine content, which possess extremely high CO_2 adsorption capacity. However, using the PSM or physical impregnation methods, we should keep in mind that the pore windows/sizes of the parent MOFs should be sufficiently large to facilitate the diffusion of amines or polyamines. Furthermore, the chemical stability of the parent MOFs should be also considered.

Upon intensive investigation during the last few years, amine-functionalized MOFs have been proven to be excellent CO_2 adsorbents. It has been demonstrated that extremely high CO_2 adsorption capacity at low pressures can be achieved *via* two routes: (i) develop amine-functionalized MOFs with narrow pore size (0.3–0.4 nm) and (ii) introduce basic alkylamines into MOFs. Nevertheless, there is still much room for improvement, such as development of amine-functionalized MOFs with both high CO_2 capacity and mild regeneration condition.

Some amine-functionalized MOFs based membranes, including pure MOFs membranes and MMMs, have been fabricated for gas separation. These membranes demonstrated advantages in CO_2/H_2, CO_2/N_2 or CO_2/CH_4 separation. It has been widely accepted that, besides the suitable pore sizes, the amino groups are responsible for the excellent CO_2 separation performance. However, research on this area is still in its infancy. Fundamental studies should remain focus on the reproducibility and stability of performance of amine-functionalized MOFs based membranes. Moreover, the scale up of amine-functionalized MOFs based membranes is a grand challenge.

Finally, some amine-functionalized MOFs have been developed as solid basic catalysts to meet the challenge in sustainable chemistry. Notably, IRMOF-3 (ref. 97) shows an excellent activity with 100% selectivity in Knoevenagel condensation of ethyl cyanoacetate and ethyl acetotacetate with benzaldehyde without diffusion limitation. NH_2-MIL-53(Al) and CAU-1 are found to be much less active. The poor activity is attributed to their narrow pore windows that limit the diffusion of reactants. Therefore, to select a suitable amine-functionalized MOF catalyst for specific reaction, pore windows of the framework should be considered. The research on amine-functionalized MOFs catalysts is just emerging and ongoing, future studies are suggested to focus on the chemical stability and recyclability of amine-functionalized MOFs catalysts under multicomponent mixtures after numerous reaction cycles.

Acknowledgements

This work is financially supported by National Key Basic Research Program of China (2013CB934800), NSFC (51272260, 51572272), NSF of Zhejiang Province (LR14E020004, LY15E020008) and the program for Ningbo municipal science and technology innovative research team (2015B11002 and 2014B81004).

References

1 H. Furukawa, U. Müller and O. M. Yaghi, *Angew. Chem., Int. Ed.*, 2015, **54**, 3417.
2 M. Eddaoudi, D. B. Moler, H. L. Li, B. L. Chen, T. M. Reineke, M. O'Keeffe and O. M. Yaghi, *Acc. Chem. Res.*, 2001, **34**, 319.

3 G. Ferey, C. Mellot-Draznieks, C. Serre, F. Millange, J. Dutour, S. Surble and I. Margiolaki, *Science*, 2005, **310**, 1119.
4 G. Ferey, *Chem. Soc. Rev.*, 2008, **37**, 191–214.
5 S. J. Garibay and S. M. Cohen, *Chem. Commun.*, 2010, **46**, 7700–7702.
6 T. Gadzikwa, O. K. Farha, K. L. Mulfort, J. T. Hupp and S. T. Nguyen, *Chem. Commun.*, 2009, 3720.
7 Y. Goto, H. Sato, S. Shinkai and K. Sada, *J. Am. Chem. Soc.*, 2008, **130**, 14354.
8 D.-M. Chen, N. Xu, X.-H. Qiu and P. Cheng, *Cryst. Growth Des.*, 2015, **15**, 961.
9 K. Liu, W. Shi and P. Cheng, *Dalton Trans.*, 2011, **40**, 8475.
10 C. Janiak and J. K. Vieth, *New J. Chem.*, 2010, **34**, 2366.
11 N. Stock and S. Biswas, *Chem. Rev.*, 2012, **112**, 933.
12 Z. Q. Wang and S. M. Cohen, *Chem. Soc. Rev.*, 2009, **38**, 1315.
13 M. E. Braun, C. D. Steffek, J. Kim, P. G. Rasmussen and O. M. Yaghi, *Chem. Commun.*, 2001, 2532.
14 M. Eddaoudi, J. Kim, N. Rosi, D. Vodak, J. Wachter, M. O'Keeffe and O. M. Yaghi, *Science*, 2002, **295**, 469.
15 K. K. Tanabe, Z. Q. Wang and S. M. Cohen, *J. Am. Chem. Soc.*, 2008, **130**, 8508.
16 J. L. C. Rowsell and O. M. Yaghi, *J. Am. Chem. Soc.*, 2006, **128**, 1304.
17 A. M. Goforth, C. Y. Su, R. Hipp, R. B. Macquart, M. D. Smith and H. C. zur Loye, *J. Solid State Chem.*, 2005, **178**, 2511.
18 B. Arstad, H. Fjellvag, K. O. Kongshaug, O. Swang and R. Blom, *Adsorption*, 2008, **14**, 755.
19 F. Vermoortele, R. Ameloot, A. Vimont, C. Serre and D. De Vos, *Chem. Commun.*, 2011, **47**, 1521.
20 Y. C. Lin, C. L. Kong and L. Chen, *RSC Adv.*, 2012, **2**, 6417.
21 J. H. Cavka, S. Jakobsen, U. Olsbye, N. Guillou, C. Lamberti, S. Bordiga and K. P. Lillerud, *J. Am. Chem. Soc.*, 2008, **130**, 13850.
22 D. M. Jiang, L. L. Keenan, A. D. Burrows and K. J. Edler, *Chem. Commun.*, 2012, **48**, 12053.
23 Y. H. Fu, D. R. Sun, Y. J. Chen, R. K. Huang, Z. X. Ding, X. Z. Fu and Z. H. Li, *Angew. Chem., Int. Ed.*, 2012, **51**, 3364.
24 M. Dan-Hardi, C. Serre, T. Frot, L. Rozes, G. Maurin, C. Sanchez and G. Ferey, *J. Am. Chem. Soc.*, 2009, **131**, 10857.
25 C. Serre, F. Millange, C. Thouvenot, M. Nogues, G. Marsolier, D. Louer and G. Ferey, *J. Am. Chem. Soc.*, 2002, **124**, 13519.
26 C. Serre, C. Mellot-Draznieks, S. Surble, N. Audebrand, Y. Filinchuk and G. Ferey, *Science*, 2007, **315**, 1828.
27 S. Couck, J. F. M. Denayer, G. V. Baron, T. Remy, J. Gascon and F. Kapteijn, *J. Am. Chem. Soc.*, 2009, **131**, 6326.
28 S. Bauer, C. Serre, T. Devic, P. Horcajada, J. Marrot, G. Ferey and N. Stock, *Inorg. Chem.*, 2008, **47**, 7568.
29 K. Peikert, F. Hoffmann and M. Froba, *Chem. Commun.*, 2012, **48**, 11196.
30 C. Lavenn, F. Albrieux, A. Tuel and A. Demessence, *J. Colloid Interface Sci.*, 2014, **418**, 234.
31 P. Serra-Crespo, E. V. Ramos-Fernandez, J. Gascon and F. Kapteijn, *Chem. Mater.*, 2011, **23**, 2565.
32 J. P. S. Mowat, S. R. Miler, J. M. Griffin, V. R. Seymour, S. E. Ashbrook, S. P. Thompson, D. Fairen-Jimenez, A. M. Banu, T. Duren and P. A. Wright, *Inorg. Chem.*, 2011, **50**, 10844.
33 J. S. Costa, P. Gamez, C. A. Black, O. Roubeau, S. J. Teat and J. Reedijk, *Eur. J. Inorg. Chem.*, 2008, 1551.
34 R. B. Lin, D. Chen, Y. Y. Lin, J. P. Zhang and X. M. Chen, *Inorg. Chem.*, 2012, **51**, 9950.
35 R. Vaidhyanathan, S. S. Iremonger, K. W. Dawson and G. K. H. Shimizu, *Chem. Commun.*, 2009, 5230.
36 T. Ahnfeldt, N. Guillou, D. Gunzelmann, I. Margiolaki, T. Loiseau, G. Ferey, J. Senker and N. Stock, *Angew. Chem., Int. Ed.*, 2009, **48**, 5163.
37 Q. J. Yan, Y. C. Lin, P. Y. Wu, L. Zhao, L. J. Cao, L. M. Peng, C. L. Kong and L. Chen, *ChemPlusChem*, 2013, **78**, 86.
38 J. An, S. J. Geib and N. L. Rosi, *J. Am. Chem. Soc.*, 2010, **132**, 38.
39 J. Y. An, S. J. Geib and N. L. Rosi, *J. Am. Chem. Soc.*, 2009, **131**, 8376.
40 J. An, O. K. Farha, J. T. Hupp, E. Pohl, J. I. Yeh and N. L. Rosi, *Nat. Commun.*, 2012, **3**, 604.
41 X. L. Si, C. L. Jiao, F. Li, J. Zhang, S. Wang, S. Liu, Z. B. Li, L. X. Sun, F. Xu, Z. Gabelica and C. Schick, *Energy Environ. Sci.*, 2011, **4**, 4522.
42 A. P. Nelson, O. K. Farha, K. L. Mulfort and J. T. Hupp, *J. Am. Chem. Soc.*, 2009, **131**, 458.
43 G. E. Cmarik, M. Kim, S. M. Cohen and K. S. Walton, *Langmuir*, 2012, **28**, 15606.
44 M. Hartmann and M. Fischer, *Microporous Mesoporous Mater.*, 2012, **164**, 38.
45 M. Savonnet, D. Bazer-Bachi, N. Bats, J. Perez-Pellitero, E. Jeanneau, V. Lecocq, C. Pinel and D. Farrusseng, *J. Am. Chem. Soc.*, 2010, **132**, 4518.
46 M. Pera-Titus, T. Lescouet, S. Aguado and D. Farrusseng, *J. Phys. Chem. C*, 2012, **116**, 9507.
47 X. Y. Chen, H. Vinh-Thang, D. Rodrigue and S. Kaliaguine, *Ind. Eng. Chem. Res.*, 2012, **51**, 6895.
48 Y. Zhang, Y. Chen, Y. P. Zhang, H. H. Cong, B. Fu, S. P. Wen and S. P. Ruan, *J. Nanopart. Res.*, 2013, **15**, 2014.
49 Z. Q. Wang, K. K. Tanabe and S. M. Cohen, *Inorg. Chem.*, 2009, **48**, 296.
50 Q. G. Zhai, Q. P. Lin, T. Wu, L. Wang, S. T. Zheng, X. H. Bu and P. Y. Feng, *Chem. Mater.*, 2012, **24**, 2624.
51 W. Kleist, M. Maciejewski and A. Baiker, *Thermochim. Acta*, 2010, **499**, 71.
52 R. B. Ferreira, P. M. Scheetz and A. L. B. Formiga, *RSC Adv.*, 2013, **3**, 10181.
53 S. Marx, W. Kleist, J. Huang, M. Maciejewski and A. Baiker, *Dalton Trans.*, 2010, **39**, 3795.
54 T. Gadzikwa, G. Lu, C. L. Stern, S. R. Wilson, J. T. Hupp and S. T. Nguyen, *Chem. Commun.*, 2008, 5493.
55 S. Bernt, V. Guillerm, C. Serre and N. Stock, *Chem. Commun.*, 2011, **47**, 2838.
56 Y. K. Hwang, D. Y. Hong, J. S. Chang, S. H. Jhung, Y. K. Seo, J. Kim, A. Vimont, M. Daturi, C. Serre and G. Ferey, *Angew. Chem., Int. Ed.*, 2008, **47**, 4144.

57 A. Demessence, D. M. D'Alessandro, M. L. Foo and J. R. Long, *J. Am. Chem. Soc.*, 2009, **131**, 8784.
58 T. M. McDonald, D. M. D'Alessandro, R. Krishna and J. R. Long, *Chem. Sci.*, 2011, **2**, 2022.
59 T. M. McDonald, W. R. Lee, J. A. Mason, B. M. Wiers, C. S. Hong and J. R. Long, *J. Am. Chem. Soc.*, 2012, **134**, 7056.
60 W. R. Lee, H. Jo, L. M. Yang, H. Lee, D. W. Ryu, K. S. Lim, J. H. Song, D. Y. Min, S. S. Han, J. G. Seo, Y. K. Park, D. Moon and C. S. Hong, *Chem. Sci.*, 2015, **6**, 3697.
61 J. S. Yeon, W. R. Lee, N. W. Kim, H. Jo, H. Lee, J. H. Song, K. S. Lim, D. W. Kang, J. G. Seo, D. Moon, B. Wiers and C. S. Hong, *J. Mater. Chem. A*, 2015, **3**, 19177.
62 Y. C. Lin, Q. J. Yan, C. L. Kong and L. Chen, *Sci. Rep.*, 2013, **3**, 1859.
63 Q. J. Yan, Y. C. Lin, C. L. Kong and L. Chen, *Chem. Commun.*, 2013, **49**, 6873.
64 Y. C. Lin, H. Lin, H. M. Wang, Y. G. Suo, B. H. Li, C. L. Kong and L. Chen, *J. Mater. Chem. A*, 2014, **2**, 14658.
65 P. L. Llewellyn, S. Bourrelly, C. Serre, A. Vimont, M. Daturi, L. Hamon, G. De Weireld, J. S. Chang, D. Y. Hong, Y. K. Hwang, S. H. Jhung and G. Ferey, *Langmuir*, 2008, **24**, 7245.
66 R. Vaidhyanathan, S. S. Iremonger, G. K. H. Shimizu, P. G. Boyd, S. Alavi and T. K. Woo, *Science*, 2010, **330**, 650.
67 Y. F. Chen and J. W. Jiang, *ChemSusChem*, 2010, **3**, 982.
68 R. Banerjee, H. Furukawa, D. Britt, C. Knobler, M. O'Keeffe and O. M. Yaghi, *J. Am. Chem. Soc.*, 2009, **131**, 3875.
69 E. Stavitski, E. A. Pidko, S. Couck, T. Remy, E. J. M. Hensen, B. M. Weckhuysen, J. Denayer, J. Gascon and F. Kapteijn, *Langmuir*, 2011, **27**, 3970.
70 K. Sumida, D. L. Rogow, J. A. Mason, T. M. McDonald, E. D. Bloch, Z. R. Herm, T. H. Bae and J. R. Long, *Chem. Rev.*, 2012, **112**, 724.
71 A. N. M. Peeters, A. P. C. Faaij and W. C. Turkenburg, *Int. J. Greenhouse Gas Control*, 2007, **1**, 396.
72 Y. Kuwahara, D. Y. Kang, J. R. Copeland, N. A. Brunelli, S. A. Didas, P. Bollini, C. Sievers, T. Kamegawa, H. Yamashita and C. W. Jones, *J. Am. Chem. Soc.*, 2012, **134**, 10757.
73 J. A. Mason, K. Sumida, Z. R. Herm, R. Krishna and J. R. Long, *Energy Environ. Sci.*, 2011, **4**, 3030.
74 F. Zhang, X. Q. Zou, X. Gao, S. J. Fan, F. X. Sun, H. Ren and G. S. Zhu, *Adv. Funct. Mater.*, 2012, **22**, 3583.
75 A. M. Fracaroli, H. Furukawa, M. Suzuki, M. Dodd, S. Okajima, F. Gandara, J. A. Reimer and O. M. Yaghi, *J. Am. Chem. Soc.*, 2014, **136**, 8863.
76 Y. Yoo and H. K. Jeong, *Cryst. Growth Des.*, 2010, **10**, 1283.
77 Y. Yoo, V. Varela-Guerrero and H. K. Jeong, *Langmuir*, 2011, **27**, 2652.
78 A. S. Huang and J. Caro, *Angew. Chem., Int. Ed.*, 2011, **50**, 4979.
79 A. S. Huang, H. Bux, F. Steinbach and J. Caro, *Angew. Chem., Int. Ed.*, 2010, **49**, 4958.
80 H. Bux, A. Feldhoff, J. Cravillon, M. Wiebcke, Y. S. Li and J. Caro, *Chem. Mater.*, 2011, **23**, 2262.
81 H. Y. Fan, H. P. Xia, C. L. Kong and L. Chen, *Int. J. Hydrogen Energy*, 2013, **38**, 10795.
82 T. Ahnfeldt, D. Gunzelmann, T. Loiseau, D. Hirsemann, J. Senker, G. Ferey and N. Stock, *Inorg. Chem.*, 2009, **48**, 3057.
83 S. Y. Zhou, X. Q. Zou, F. X. Sun, H. Ren, J. Liu, F. Zhang, N. Zhao and G. S. Zhu, *Int. J. Hydrogen Energy*, 2013, **38**, 5338.
84 N. Y. Wang, A. Mundstock, Y. Liu, A. S. Huang and J. Caro, *Chem. Eng. Sci.*, 2015, **124**, 27.
85 J. A. Bohrman and M. A. Carreon, *Chem. Commun.*, 2012, **48**, 5130.
86 H. M. Yin, J. Q. Wang, Z. Xie, J. H. Yang, J. Bai, J. M. Lu, Y. Zhang, D. H. Yin and J. Y. S. Lin, *Chem. Commun.*, 2014, **50**, 3699.
87 E. Atci, I. Erucar and S. Keskin, *J. Phys. Chem. C*, 2011, **115**, 6833.
88 T. S. Chung, L. Y. Jiang, Y. Li and S. Kulprathipanja, *Prog. Polym. Sci.*, 2007, **32**, 483.
89 Y. F. Zhang, I. H. Musseman, J. P. Ferraris and K. J. Balkus, *J. Membr. Sci.*, 2008, **313**, 170–181.
90 T. H. Bae, J. S. Lee, W. L. Qiu, W. J. Koros, C. W. Jones and S. Nair, *Angew. Chem., Int. Ed.*, 2010, **49**, 9863–9866.
91 S. Basu, A. Cano-Odena and I. F. J. Vankelecom, *J. Membr. Sci.*, 2010, **362**, 478–487.
92 B. Zornoza, A. Martinez-Joaristi, P. Serra-Crespo, C. Tellez, J. Coronas, J. Gascon and F. Kapteijn, *Chem. Commun.*, 2011, **47**, 9522.
93 L. M. Robeson, *J. Membr. Sci.*, 1991, **62**, 165–185.
94 O. G. Nik, X. Y. Chen and S. Kaliaguine, *J. Membr. Sci.*, 2012, **413**, 48.
95 L. J. Cao, K. Tao, A. S. Huang, C. L. Kong and L. Chen, *Chem. Commun.*, 2013, **49**, 8513.
96 M. J. Ingleson, J. P. Barrio, J. B. Guilbaud, Y. Z. Khimyak and M. J. Rosseinsky, *Chem. Commun.*, 2008, 2680.
97 J. Gascon, U. Aktay, M. D. Hernandez-Alonso, G. P. M. van Klink and F. Kapteijn, *J. Catal.*, 2009, **261**, 75.
98 A. R. Burgoyne and R. Meijboom, *Catal. Lett.*, 2013, **143**, 563–571.
99 M. Savonnet, S. Aguado, U. Ravon, D. Bazer-Bachi, V. Lecocq, N. Bats, C. Pinel and D. Farrusseng, *Green Chem.*, 2009, **11**, 1729.
100 W. Kleist, F. Jutz, M. Maciejewski and A. Baiker, *Eur. J. Inorg. Chem.*, 2009, 3552.
101 D. Y. Hong, Y. K. Hwang, C. Serre, G. Ferey and J. S. Chang, *Adv. Funct. Mater.*, 2009, **19**, 1537.
102 S. J. Garibay, Z. Q. Wang and S. M. Cohen, *Inorg. Chem.*, 2010, **49**, 8086.